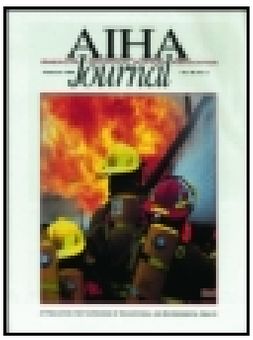

AIHAJ - American Industrial Hygiene Association

ISSN: 1529-8663 (Print) (Online) Journal homepage: https://www.tandfonline.com/loi/uaah20

Mechanistic Understanding of Aerosol Emissions from a Brazing Operation

Anthony T. Zimmer & Pratim Biswas

To cite this article: Anthony T. Zimmer & Pratim Biswas (2000) Mechanistic Understanding of Aerosol Emissions from a Brazing Operation, AIHAJ - American Industrial Hygiene Association, 61:3, 351-361, DOI: 10.1080/15298660008984543

To link to this article: https://doi.org/10.1080/15298660008984543

Mechanistic Understanding of Aerosol Emissions from a Brazing Operation

AUTHORS
Anthony T. Zimmer[a,b]
Pratim Biswas[a]

[a]Aerosol and Air Quality Research Laboratory, Department of Civil and Environmental Engineering, University of Cincinnati, Cincinnati, Ohio 45221–0071; [b]National Institute for Occupational Safety and Health, Division of Physical Sciences and Engineering, 4676 Columbia Parkway, R5, Cincinnati, Ohio 45226

Welding operations produce gaseous and aerosol by-products that can have adverse health effects. A laboratory furnace study was conducted to aid understanding of the chemical and aerosol behavior of a widely used, self-fluxing brazing alloy (89% Cu, 6% Ag, 5% P) that is also used with a supplemental fluxing compound to prevent oxidation at the molten metal surface. The results indicate that the aerosols generated by the alloy are transient (produced over a short duration of time) and are associated with mass transfer of phosphorus species from the molten metal surface to the surrounding gas. In contrast, when the alloy was used in conjunction with the supplemental fluxing compound, a relatively nontransient, submicron-size aerosol was generated that was several orders of magnitude higher in concentration. Thermodynamic equilibrium analysis suggests that fluoride (a major constituent in the fluxing compound) played a significant role in reacting with the brazing alloy metals to form gas phase metal fluoride compounds that had high vapor pressures when compared with their elemental or oxide forms. As these metal-fluoride vapors cooled, submicron-size particles were formed mainly through nucleation and condensation growth processes. In addition, the equilibrium results revealed the potential formation of severe pulmonary irritants (HF and BF_3) from heating the supplemental fluxing compound. These results demonstrated the importance of fluxing compounds in the formation of brazing fumes, and suggest that fluxing compounds could be selected that serve their metallurgical intention and suppress the formation of aerosols.

Keywords: aerosols, brazing, chemical, equilibrium analysis fumes, welding

There are more than 80 different types of welding processes, and each process uses a wide variety of alloys and fluxing agents.[1] Welding operations produce gaseous and aerosol by-products composed of a complex array of metals, metal oxides, and other chemical species volatilized from either the base metal, the welding electrode, or the flux material.[2–4] Census data indicates that over 700,000 workers in the United States are involved in welding or allied processes.[5] Animal and epidemiological studies suggest that welding is associated with a wide range of adverse health effects such as metal fume fever, pneumonitis, chronic bronchitis, and decrements in pulmonary function.[2] A large body of evidence suggests that welders generally have high numbers of respiratory cancer.[2] Welding processes are known to generate aerosols with a significant fraction in the nanometer size range.[3,6,7] Recent research also has indicated that particles in the nanometer size range may have adverse health effects.[8–10]

The health effects due to welding fume exposures depend on several factors. One important factor is the chemical speciation, formation, and growth processes of the particles. This depends on several parameters such as the welding process, the operational temperatures, and the composition of constituents in the base metal, filler materials, and fluxing agents. Several aerosol studies in the literature[3,6,7] have examined arc welding fume formation processes. These studies found that the method used to protect the molten metal surface against oxidation had a significant effect on the characteristics of the arc welding fume. Based on cascade impactor data, 100% of the shielded metal arc welding (SMAW) fumes were

less than 1 μm aerodynamic equivalent diameter (AED), and nearly 100% of the gas metal arc welding (GMAW) fumes were below 0.5 μm AED.[3,7] Hewett[7] reported that the fumes generated from these processes had significant differences in the density (GMAW>SMAW), specific surface areas (GMAW>SMAW), and particle size (GMAW<SMAW). Heile and Hill[6] found similar size differences in the fumes formed from these processes. Although a body of information is available on the fume emissions from certain types of arc welding operations, limited data[3] exists for new technologies and established processes such as soldering and brazing.

Brazing operations are similar to soldering, although the melting point of the filler metal is higher (>450°C). Using heat sources such as furnaces and torches, brazing is used to join metals by melting a filler metal.[1] Brazing is extensively used to join copper, especially tubing for refrigeration and air conditioning applications.[11] An alloy, composed of the base metal and several other ingredients, is used to lower the alloy melt point, which facilitates wettability and flowability. Cadmium-copper alloys were extensively used to obtain these characteristics. However, when the Occupational Safety and Health Administration lowered its cadmium exposure limits standard in 1992, the industry was forced to adopt alternative alloys.[12] Copper-phosphorus alloys were adopted as one alternative,[12,13] and the addition of phosphorus lowered the melt temperature, increased the fluidity, and also acted as a deoxidant/fluxing agent for copper. While the role of phosphorus from a brazing and metallurgical viewpoint is relatively well understood, the resultant fume generation characteristics have not been reported.

The formation of the fume in welding and brazing processes is analogous to that of aerosol formation in a combustion system.[14] The fume formation characteristics are strongly dependent on the chemical speciation. In several engineering applications, thermodynamic equilibrium analysis has been employed successfully as a qualitative assessment tool in evaluating the form and phase (condensed or gaseous) of metals encountered in waste incineration processes. Wu and Biswas[15] used this technique to determine the speciation and phase (i.e., solid, liquid, or gas) of metals in an incinerator. Fernandez et al.[16] applied thermodynamic equilibrium analysis to categorize heavy metals in the combustion gases of urban waste incinerators. Durlak et al.[17] evaluated the role of process parameters on metallic emission rates. Owens et al.[18] used this technique to determine the feasibility of using sorbents to control toxic metal emissions and to identify optimal operating regimes for maximal removal of metallic species. The application of this technique to welding processes could yield valuable information regarding the form and phase of the welding fume. A means of predicting the form of a chemical species (e.g., Cr(IV) or Cr(VI)) would be important from a toxicological standpoint, and the phase of chemical species also would allow one to infer the aerosol forming potential, which is also species dependent.

Although the health effects of welding fumes are well documented,[2] relatively few studies have focused on the formation and growth characteristics of welding fumes,[3,6,7] especially for brazing and soldering applications.[19] This article reports on the results of a laboratory furnace study to evaluate the chemical and aerosol dynamics of a self-fluxing brazing alloy that can be used both individually and with a supplemental fluxing compound. This study represents one of the few attempts to fundamentally characterize the aerosol behavior of a brazing alloy. To assist in interpreting the furnace study results, thermodynamic equilibrium analysis was used to predict the chemical species that are favored when this alloy is used by itself and when the alloy is used with the supplemental fluxing compound. Fundamental understanding of the factors that influence the formation of brazing fumes should provide insight regarding its control.

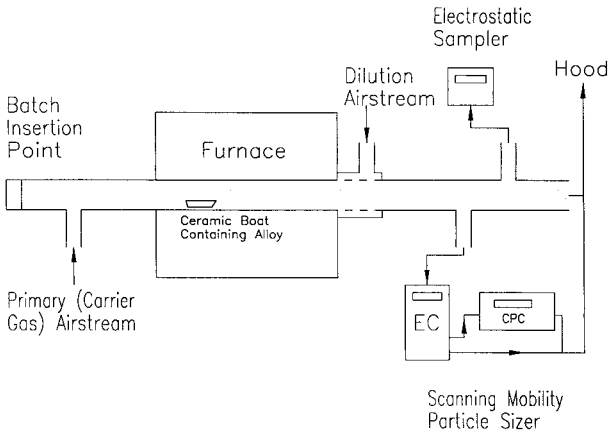

FIGURE 1. Schematic diagram of the experimental setup

METHODOLOGY

A widely used copper-phosphorus-silver brazing alloy[13] was selected for study. The brazing alloy has a melting point of 643°C (flow point 732°C) and is composed of 89% Cu, 5% Ag, and 6% P. As stated, this alloy is self-fluxing and can be used by itself when joining copper materials. When the base metals are dirty or when brazing other alloys (e.g., brass or bronze), a supplemental fluxing compound is frequently used. The fluxing compound further assists in protecting the metal against oxidation, and contains the following primary ingredients: 30–60% H_3BO_3, 25–40% KF_2, and 15–25% H_2O. Information regarding the composition of the alloy and fluxing compound was obtained from the manufacturer's material safety data sheets (J.W. Harris Co., Inc., Cincinnati, Ohio). The following sections describe the approach used to experimentally study the fumes generated by this alloy. Also described is the method used for the equilibrium calculations and the simulation conditions to evaluate the behavior of the brazing alloy metal when used by itself and in conjunction with the fluxing compound.

Experimental System and Plan

To simulate a brazing process, an experimental system was designed as illustrated in Figure 1. To determine an appropriate temperature range for the furnace brazing experiments, temperature profiles were measured during a torch brazing operation. The temperature adjacent to the molten pool varied as the torch was moved, with a maximum measured temperature of 700°C, although the temperature at the molten pool surface was likely higher from contact with the flame.[20] A system consisting of a 2.54 cm (1 inch) i.d. alumina tubular flow reactor maintained at selected temperatures by a Lindbergh tube furnace (model HTF55342C, T_{max} = 1200°) was used to simulate the brazing process. The metal alloy (and/or fluxing compound) was placed in a ceramic boat that was inserted into the high temperature region of the furnace. In all batch experiments, the dimensions of the alloy piece were 4.0 × 0.1 × 0.3 cm (mass = 1.18 ± 0.02

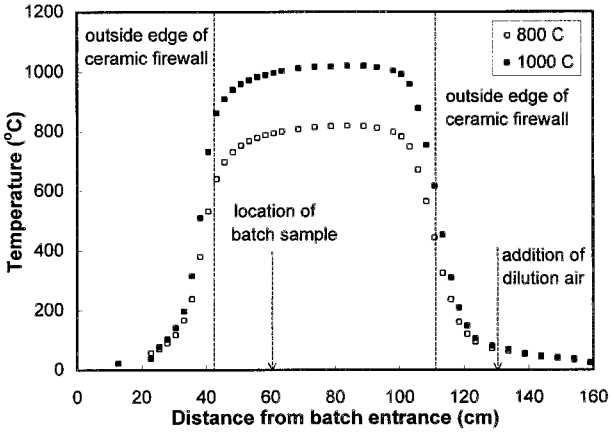

FIGURE 2. Measured temperature profile in the furnace reactor for two set points

g). Figure 2 illustrates the temperature profile of the furnace, location of the alloy sample, and addition of the dilution air. Brazing operations are conducted under a wide range of conditions, from an uncontrolled environment (e.g., brazing on a refrigeration system at a new/existing building) to a well-controlled environment (e.g., brazing in an industrial refrigeration assembly operation). In this experimental study, the velocity of the carrier gas passing over the molten metal was selected to simulate brazing in a relatively quiescent environment.

A primary gas-stream, composed of particle-free air (approximately 80% nitrogen and 20% oxygen) or inert gas (100% nitrogen), was passed over the molten metal surface, allowing elements within the alloy to volatilize into the gas stream. As this gas stream approached the exit of the reactor, the temperature rapidly decreased (Figure 2), resulting in conditions that favored the formation of an aerosol. A dilution apparatus was designed to introduce dilution air as the gas stream exited the heated portion of the reactor. The dilution air was used to introduce dilution air at the outlet of the furnace. It quenched the aerosol dynamics and chemical reactions that could have taken place in the sample line.[21] This resulted in a representative measurement of the constituents shortly after emission. Additionally, dilution air simulated the quenching that occurs in a brazing operation. In this study, the carrier gas flow rate was maintained at 1 L/min, while the dilution flow rate was maintained at 4 L/min (using particle-free air).

Following the dilution, aerosol measurements were taken by directing a slipstream to a condensation particle counter (CPC) (TSI Inc., St. Paul, Minn., model 3022A) or a scanning mobility particle sizer (SMPS) (TSI Inc., Differential Mobility Analyzer, model 3934 and CPC, model 3022A). The CPC was used to measure particle number concentration in real-time. The SMPS was used to measure the particle size number distribution of aerosols based on the electrical mobility of the particles. From these data, information on mean particle size and deviation, particle number concentration, total particle surface area concentration, and total particle volume concentration could be determined. The SMPS required approximately 2 min to measure a particle size distribution in the nanometer size regime.[22] Because of the time requirements of the SMPS, the CPC was first used to characterize transitory aerosol behavior on heating the brazing alloy. In addition to the direct-reading aerosol instrumentation, several techniques were used to analyze the chemical behavior and morphology of the brazing alloy and fluxing compound. X-ray diffraction (XRD) (Siemens model D500) was used to evaluate the coatings that had formed on the alloy surface. Particle morphology was characterized by transmission electron microscopy (TEM) (Philips, model 420), coupled with energy dispersive X-ray analysis (model EM420), to determine the elemental composition of the particles. TEM samples were collected by directing a slipstream to an electrostatic aerosol sampler (TSI Inc., model 3100).

To study the aerosol formation and growth processes, a series of measurements were conducted, as listed in Table I. The initial experiments were conducted using the brazing alloy over a wide range of temperatures (700 to 1000°C) using particle-free air (Test I) and an inert gas (nitrogen) (Test II). The total particle number concentration was monitored with respect to time using the CPC. The total number concentration fluctuated with time (as discussed later). To characterize this transient behavior, a detailed set of measurements were carried out (Test III). A series of additional experiments (Test IV through VIII) were conducted to evaluate the role of the supplemental fluxing compound in the aerosol generation and growth characteristics.

Equilibrium Analysis and Simulation Conditions

Thermodynamic equilibrium calculations are based on a method that directly minimizes Gibbs free energy, subject to constraints on the total number of moles of each element in a system.[23] This technique was used to determine the phase (condensed and gas) and concentration of chemical species that may form on heating the alloy (or alloy and fluxing compound) in the presence of particle-free air. It must be emphasized that this approach is used to obtain equilibrium (steady-state) values. In a real system, the behavior of the alloy during an actual brazing operation will depend on a variety of factors, including mass transfer rates and chemical kinetic processes. For example, during arc welding operations, lack of ideality results in that mass transfer not only includes vaporization of the electrode constituents, but spatter from the electrode directly to the

TABLE I. List of Experiments Performed

Test	Analytical Technique	Carrier Gas[A]	Batch Sample Type	Furnace Temperatures (°C)
I	CPC	air	alloy	700, 800, 900, 1000
II	CPC	nitrogen	alloy	700, 800, 900, 1000
III	SMPS, XRD, TEM	air	alloy	900
IV	CPC	air	alloy & flux	900
V	SMPS, TEM	air	alloy & flux	900
VI	SMPS	air	flux	900
VII	SMPS	air	alloy & flux	700
VIII	SMPS	air	flux	700

[A]Carrier gases are particle-free.

TABLE II. Equilibrium Analysis Simulation Conditions for the Brazing Alloy (Case A), and the Brazing Alloy Used in Conjunction with the Fluxing Compound (Cases B–E)

Element	Case A	Case B	Case C	Case D	Case E
Oxygen	0.2	0.2	0.2	0.2	0.2
Nitrogen	0.8	0.8	0.8	0.8	0.8
Copper	10^{-6}	10^{-6}	10^{-6}	10^{-6}	10^{-6}
Silver	10^{-6}	10^{-6}	10^{-6}	10^{-6}	10^{-6}
Phosphorus	0, 10^{-3}, 10^{-2}	10^{-3}	10^{-3}	10^{-3}	10^{-3}
Boron	0	10^{-6}	10^{-6}	10^{-6}	10^{-6}
Potassium	0	10^{-6}	10^{-6}	10^{-6}	10^{-6}
Fluoride	0	10^{-6}	10^{-5}	10^{-5}	10^{-5}
Hydrogen	0	0	0	10^{-6}	10^{-5}

Note: Amounts are in moles.

ambient environment.[24] The high temperatures encountered during welding operations assists the equilibrium assumption in that reaction rates tend to vary exponentially with temperature.[25] In this work, the equilibrium calculations were performed using a computer code, STANJAN.[26] The required thermodynamic data was obtained from JANAF,[27] and compiled by Wu and Biswas.[15] Thermodynamic data for several metal fluoride species were added to the database to account for these species.[20]

To conduct a thermodynamic equilibrium analysis, the appropriate input conditions must be determined. To determine the input conditions for the brazing alloy and supplementary fluxing compound, a relation needs to be developed between the elements vaporizing from the molten metal surface (moles/time) and the air that is flowing past the molten metal surface (moles/time). This relation can be determined using a mathematical mass transfer relationship, or can be ascertained from experimental measurements. The latter approach was used in that aerosol size distribution measurements (particle number concentration and volume mean particle diameter) were used to make an order of magnitude approximation for this relation. Table II presents the simulation cases used to evaluate the speciation of the metals in the brazing alloy when used by itself (Case A), and when the alloy was used in conjunction with elements found in the fluxing compound (Cases B–E). The composition of the air was the same as that of the furnace study (20% O_2 and 80% N_2). Case A served to simulate the speciation of the silver and copper when subjected to varying quantities of phosphorus. In Cases B-E, the metals in the fluxing compound (i.e., B and K) were assumed to be on the same order of magnitude as that of the alloy metals (10^{-6}). In Cases B and C, fluoride was incorporated into the simulation matrix to determine its effect on the metals found in the alloy and fluxing compound. In Case B, fluoride was added at quantities equal to that of the metals to determine the affinity of each metal for fluoride. In Case C, fluoride was added to the simulation matrix in excess quantities. In a similar manner, Cases D and E were used to test the effect of hydrogen on the speciation of the metals. In both cases fluoride was held in excess quantities as compared with the metals. The temperature range selected for the different cases was 650 to 1300°C, to represent temperatures at the alloy melt-point to temperatures below adiabatic flame temperatures. One hundred and twenty chemical species were predicted a priori to represent possible species gaseous and aerosol by-products from the brazing process. The number of chemical species evaluated depended on whether an element was initially present during the simulation case.[20]

RESULTS AND DISCUSSION

Furnace Study

The results of the alloy-only experiments are discussed first, followed by a discussion of the alloy and flux experiments.

Metal Alloy Behavior

The first set of experiments (Test I) was conducted using air (particle-free) as the primary carrier gas over a range of temperatures (700 to 1000°C, Table I). The total number concentrations measured by the CPC at the outlet are plotted as a function of time in Figure 3 for the various temperatures. At all temperatures, the number concentration increased and gradually decreased to background concentrations. For a furnace temperature of 700°C, the number concentration attained a peak value of 3×10^5 particles per cubic centimeter of air (particles $\times$ cm^{-3}) in approximately 100 sec, a characteristic of the batch operation conducted. The time to attain the first peak concentration was approximately the same at all temperatures (Figures 3a, 3b, 3c, 3d), further confirming that this was the time for the first aerosol parcel to reach the CPC. The number concentration then gradually dropped off to background levels (<10 particles $\times$ cm^{-3}) at 300 to 400 sec after the start of the batch experiment (Figure 3a). This may have been due to the quick vaporization of a constituent that stopped after a short time. The transient behavior also was observed for the 800°C experiment (Figure 3b). In this case, however, there appeared to be a plateau observed (between 200 to 600 sec) after the decay of the first peak, with a lower total number concentration ($\sim 1 \times 10^5$ particles $\times$ cm^{-3}). This was probably indicative of volatilization of another constituent resulting in different aerosol behavior. It should be noted that the first peak number concentration was higher at 800°C compared with 700°C, due to greater volatilization. This trend also was observed at 900 and 1000°C: The first peak concentration increased and the time period over which the plateau was observed also increased. The increased first peak concentration (from 3×10^5 particles $\times$ cm^{-3} at 700°C to 1×10^7 particles $\times$ cm^{-3} at 1000°C) was due to faster volatilization resulting in higher nucleation rates. The increased concentration also may have been due to the higher temperature gradients at the reactor exit resulting in higher nucleation rates. The plateau observed for the higher temperature sample tests clearly indicates that the chemical behavior of the molten alloy changes with respect to time, and thus the measured number concentrations. Detailed experiments were performed to elucidate this behavior, and the results are discussed later in this article.

To examine whether the chemistry was altered due to reactions with air, experiments were conducted in an inert gas (i.e., nitrogen) (Test II); the results are plotted in Figure 4. Only one peak was observed at all temperatures (Figures 4a through 4d), and the transient behavior was nearly the same at all temperatures (including similar peak number concentrations, $\sim 1 \times 10^7$ particles $\times$ cm^{-3}). Thus, the plateau observed after approximately 300 to 400 sec at higher temperature tests (Figures 3b, 3c, 3d) in air were clearly due to alteration of the molten metal chemistry due to interaction with oxygen in air.

To further elucidate the mechanistic behavior, a detailed characterization was carried out for the 900°C case (Test III, Table I). The CPC measurement (Figure 3c) indicated that there were three distinct time periods: (1) from 0 to 200 sec, wherein the particle number concentration reached a peak value and decayed; (2) from 200 to 575 sec, wherein a plateau in the total number concentration was observed, and (3) from 575 to 800 sec, wherein

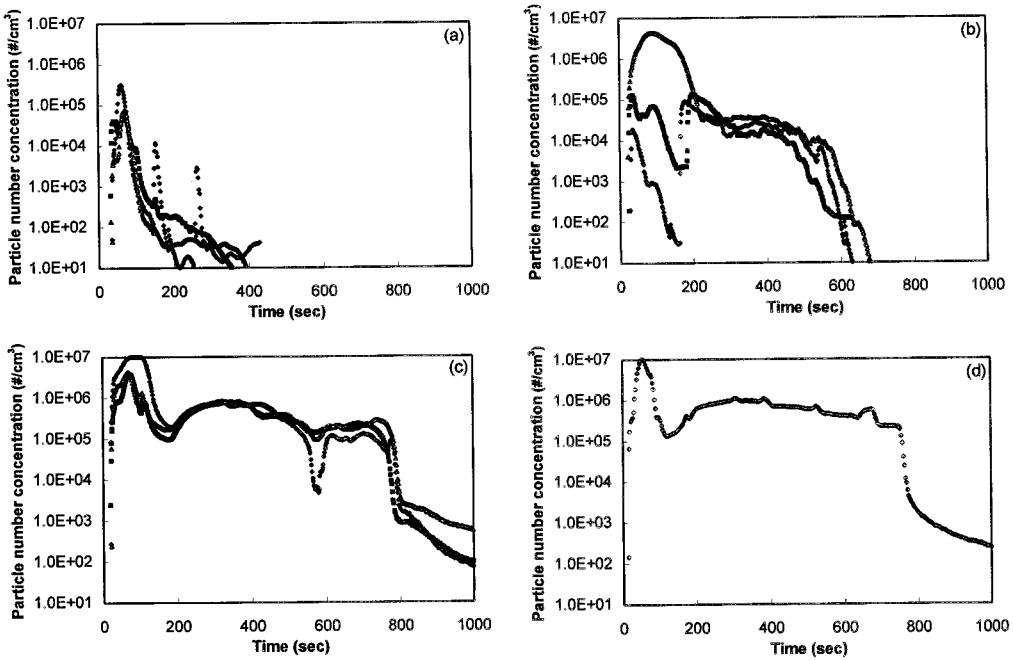

FIGURE 3. Total particle number concentrations measured by the CPC at various temperatures in air: (a) 700°C, (b) 800°C, (c) 900°C, and (d) 1000°C (different symbols on each graph represent replicate measurements)

another plateau (lower number concentration) was observed that rapidly decayed to background levels. The XRD patterns of material removed from the upper layers of the batch samples for each of these time periods are shown in Figure 5. A search of the Joint Committee on Powder Diffraction Standards (JCPDS) library revealed the presence of elemental copper. Several additional peaks were observed; unfortunately, they could not be identified using this library. These peaks could be representative of Ag/P compounds. As seen in Figure 5, heating markedly changed the chemistry of the alloy coating. Heating the alloy up to 200 sec revealed the presence of copper phosphate ($Cu_2P_2O_7$). In addition, the peaks corresponding to elemental copper were still present. Although not shown on the figure, the JCPDS library search also suggested the presence of silver phosphate ($Ag_4P_2O_7$, with characteristic peaks evident at 2-theta angles corresponding to 32.57 and 38.37°). The alloy had partially melted and a gray coating had formed on the alloy surface. In evaluating the sample corresponding to heating from 200 to 575 sec, the copper phosphate peaks were still clearly present. In the coating corresponding to 575 to 800 sec, XRD analysis showed the presence of copper oxide. At times corresponding to greater than 800 sec, the XRD results indicated pronounced copper oxide peaks confirming further conversion to copper oxide.

In contrast to the above observations, the surface layers for the nitrogen tests (Test II) had a very different color and texture (clearly different in appearance from the copper phosphate or copper oxide layer). The surface of the sample was very hard (potentially a nitride) and could not be removed to perform XRD analysis.

The SMPS was used to characterize the aerosol size distribution within the three time periods observed with the CPC. Measurements at times ranging from 0 to 200 sec did not reveal observable particle size distributions, although particles were clearly detected by the CPC (Figure 3c). One possible reason is that the particles were larger than the upper limit of the SMPS measurement (420 nm) or were removed in the upstream impactor (cut-off size = 457 nm). However, a close examination reveals that the number of particles decreases with increasing size (Figure 6), and this is not possibly the reason. A more probable reason is that the particles are below the size range for optimal detection by the SMPS. A review of the operating principles of the SMPS shows that the charge efficiency of the electrostatic classifier markedly decreases as the particle size decreases.[28] Assuming a particle size of 20 nm, the charging efficiency for the electrostatic classifier is ~1.6%. Conversely, the detection efficiency for the CPC at this particle size is greater than 90%.[29] Though this is accounted for in the inversion routine used, the differential mobility analyzer may not be very accurate (in comparison with the CPC) in quantitatively detecting the ultrafine particles. The SMPS measurements from 200 to 575 sec revealed a particle size distribution with a total number concentration of 4400 particles $\times$ cm^{-3}, a number mean diameter of 45 nm, and a geometric standard deviation, s_g equal to 1.36 (see Figure 6 and Table III). The SMPS tests conducted from 575 to 800 sec still revealed a similar distribution, (d_{mean} = 46 nm, s_g = 1.47), with lower number concentrations (N_o = 606 particles $\times$ cm^{-3}). The XRD results described earlier (Figure 5) indicate that the aerosol particles may have been copper phosphate, which volatilized from the surface. After 575 sec the copper oxide becomes the dominant species, and the aerosol concentrations decrease due to its lower volatility. The detailed SMPS results for these measurements, and additional measurements discussed later in this work, were reported in Zimmer.[20]

Under conditions similar to those of the SMPS measurements over the different time periods, samples were collected on TEM grids. Multiple runs were used to ensure that sufficient particles were collected at time periods corresponding to the three peaks noted in Test I (Figure 3c). As stated earlier, no particles were observed at times less than 200 sec when using the SMPS. An

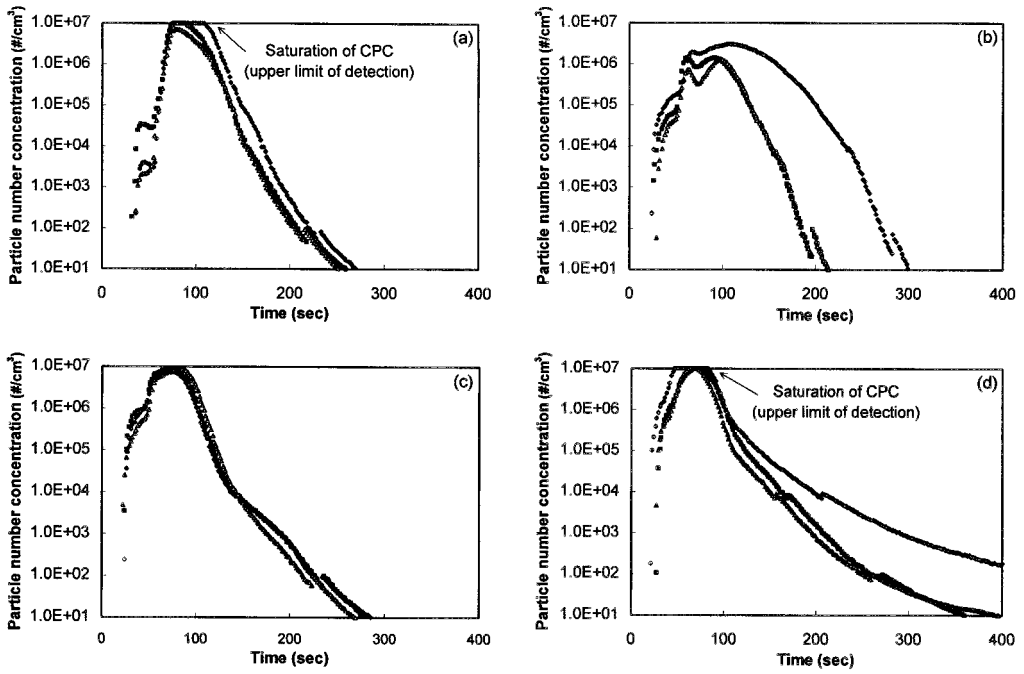

FIGURE 4. Total particle number concentrations measured by the CPC at various temperatures in nitrogen: (a) 700°C, (b) 800°C, (c) 900°C, and (d) 1000°C (different symbols on each graph represent replicate measurements)

analysis of the TEM grids for this time interval were consistent with the SMPS results in that several nearly spherical submicron particles with diameters less than 20 nm (no attempt was made to characterize the size distribution due to an insufficient number of particles on the grid) were present. TEM grid samples corresponding to a time interval of 200 to 575 sec revealed the presence of several nearly spherical submicron particles with diameters less than 100 nm (again, no attempt was made to characterize the size

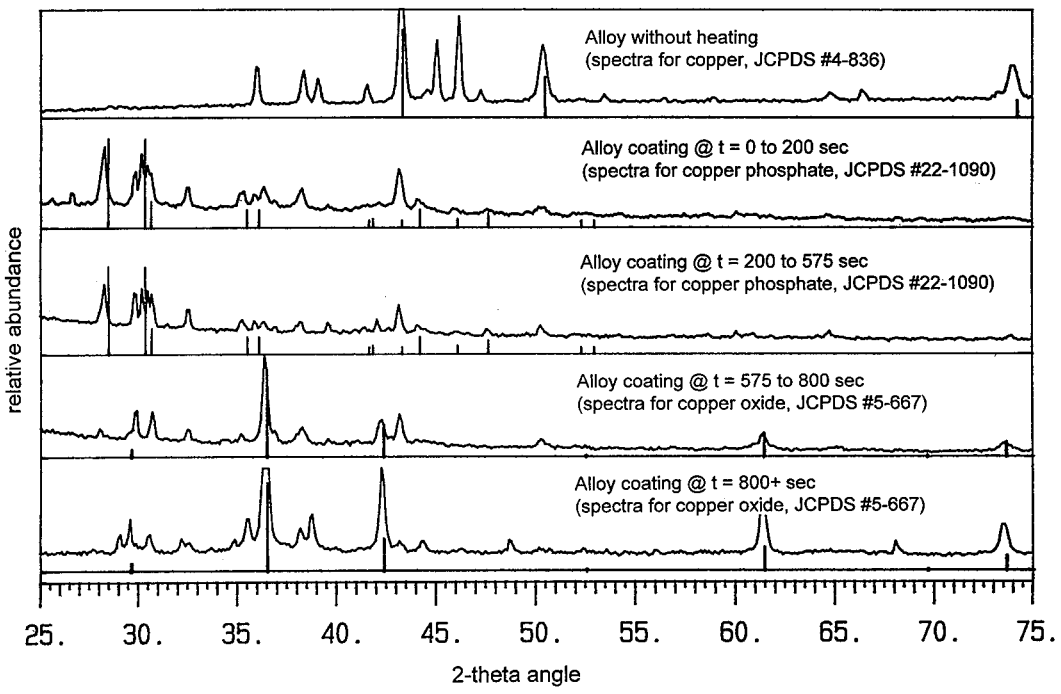

FIGURE 5. X-ray diffraction analysis of the brazing alloy surface at 900°C as a function of varying time in the furnace (curves represent the actual diffraction analysis and the underlying spectra identify characteristic peaks associated with a probable chemical species)

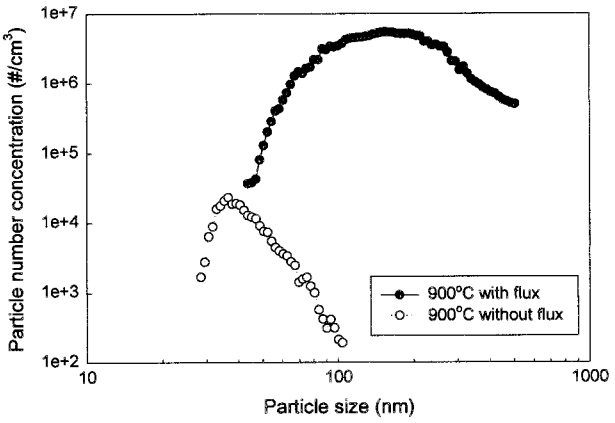

FIGURE 6. Aerosol size distributions measured by the SMPS at 900°C for the brazing alloy by itself (CPC times corresponding to 200–575 sec), and the brazing alloy with the supplemental fluxing compound

distribution due to a lack of sufficient particles on the grid). This finding is also consistent with the SMPS measurements for this time interval. The TEM samples corresponding to a time interval from 575 to 800 sec did not reveal the presence of particles. The low particle number concentrations during this time interval made it difficult to get particles onto the TEM grids. Although nickel TEM grids were used, copper present in the TEM sample holder prevented the identification of copper-containing particles using energy dispersive X-ray analysis. Particles containing silver could not be found on any of the TEM samples, although the presence of phosphorus was confirmed on the TEM grid corresponding to a time interval of 200–575 sec.

The sample results conducted using the self-fluxing brazing alloy show that the formation of aerosols is transitory and associated with distinct chemical changes occurring at the molten metal surface. It is hypothesized that when the alloy is initially heated, elemental phosphorus quickly volatilizes from the alloy surface and reacts with oxygen to form extremely small particles. In addition, the phosphorus also reacts chemically in the molten brazing alloy with the elemental copper and silver to form a metal phosphate species. These species tend to volatilize after the quick vaporization of the elemental phosphorus, and produce aerosols that have lower total particle number concentrations and larger mean particle (mobility equivalent) diameters. As time progresses, the phosphorus near the molten metal surface is consumed, allowing the oxygen in the surrounding gas to attack the surface to form copper oxide. Because the oxide has a low vapor pressure at these temperatures, mass transfer from the molten metal surface to the surrounding gas is effectively stopped, thus blocking the formation of an aerosol. In an actual brazing operation, the formation of an oxide is highly undesirable because it severely weakens the weld joint. The aerosols observed in this study, particularly those observed during the initial heating of the self-fluxing brazing alloy, should resemble those encountered during actual brazing operations.

TABLE III. Summary of Size Distribution Measurements Using the SMPS

Sample (Test #)	Temp (°C)	N_o (#/cm³)	d_p (nm)	σ_g	Comments
Alloy (III)	900	4.4×10^3	45	1.36	transient
Alloy & flux (V)	900	2.3×10^6	201	1.47	600+ sec
Flux (VI)	900	1.4×10^4	111	1.48	transient
Alloy	700	nd	nd	nd	
Alloy & flux (VII)	700	1.3×10^5	117	1.85	600+ sec
Flux (VIII)	700	nd	nd	nd	

Note: nd = not detected.

Metal Alloy and Flux Behavior

The behavior of the alloy at 900°C (Test IV, Table I) resulted in an aerosol with high number concentrations ($>1 \times 10^8$ particles $\times$ cm^{-3}) for extended periods (greater than 15 min). Even after significant dilution of the primary gas, the total number concentration was much greater than the upper detection limit for the CPC (1×10^8 particles $\times$ cm^{-3}).

The "alloy and flux" (Test IV) result was very different from that of the "alloy only" (Test I) result. The alloy-only test resulted in a transient aerosol as reported earlier. In contrast, the addition of the flux resulted in more volatilization from the molten metal surface, creating a relatively stable aerosol. Based on CPC results for the alloy and fluxing compound, Test V (Table I) was conducted to characterize the aerosol size distribution at 900°C. Based on the SMPS measurements, the total number concentration was significantly higher (2.3×10^6 particles $\times$ cm^{-3}), and the number mean particle diameter was larger (201 nm) (Figure 6 and Table III). During this test, the aerosol behavior remained relatively constant for greater than 600 sec.

To elucidate the role of the fluxing compound, the size distribution of the "flux only" (Test VI) experiment was measured. A transient aerosol with a total number concentration of 1.4×10^4 particles $\times$cm^{-3} and a number mean diameter of 111 nm was observed for approximately 180 sec. On comparing these results with those of Test V, it is clear that the flux-metal alloy combination resulted in greater volatilization of the metallic constituents, a fact corroborated by the TEM measurements and the results of the equilibrium analysis discussed later. The larger mean diameter in Test V is probably due to condensational growth of the nucleated particles.

The increased volatility of the metal alloy constituents due to reaction with the fluxing compounds is confirmed by carrying out tests with the "alloy and flux" (Test VII) and "flux only" (Test III) at a lower temperature (700°C). The results of the "metal alloy only" (Test I) reported earlier resulted in transient behavior (backgrounds concentrations reached after approximately 200 sec), and no measurable size distribution using the SMPS. The "flux only" (Test VIII) sample results yielded no measurable size distributions at 700°C. However, the "metal alloy and flux" resulted in a measurable size distribution for more than 600 sec. The number mean particle diameter was lower than in the corresponding 900°C test due to a lower rate of volatilization and condensational growth.

In addition to size distribution measurements at 900°C, TEM samples were collected to evaluate the morphology and chemical composition of the aerosols generated from the "alloy and flux" (Test V). Figure 7 is a photograph of the fumes generated under these conditions. The aerosol particles were mainly spherical in shape, with particle diameters ranging from 50 to 300 nm. These diameters were consistent with those of the SMPS results. As explained previously, copper could not be identified using energy dispersive X-ray analysis. However, other elements in the brazing alloy and fluxing compound such as silver, phosphorus, and potassium were identified. Elements such as fluorine and boron could

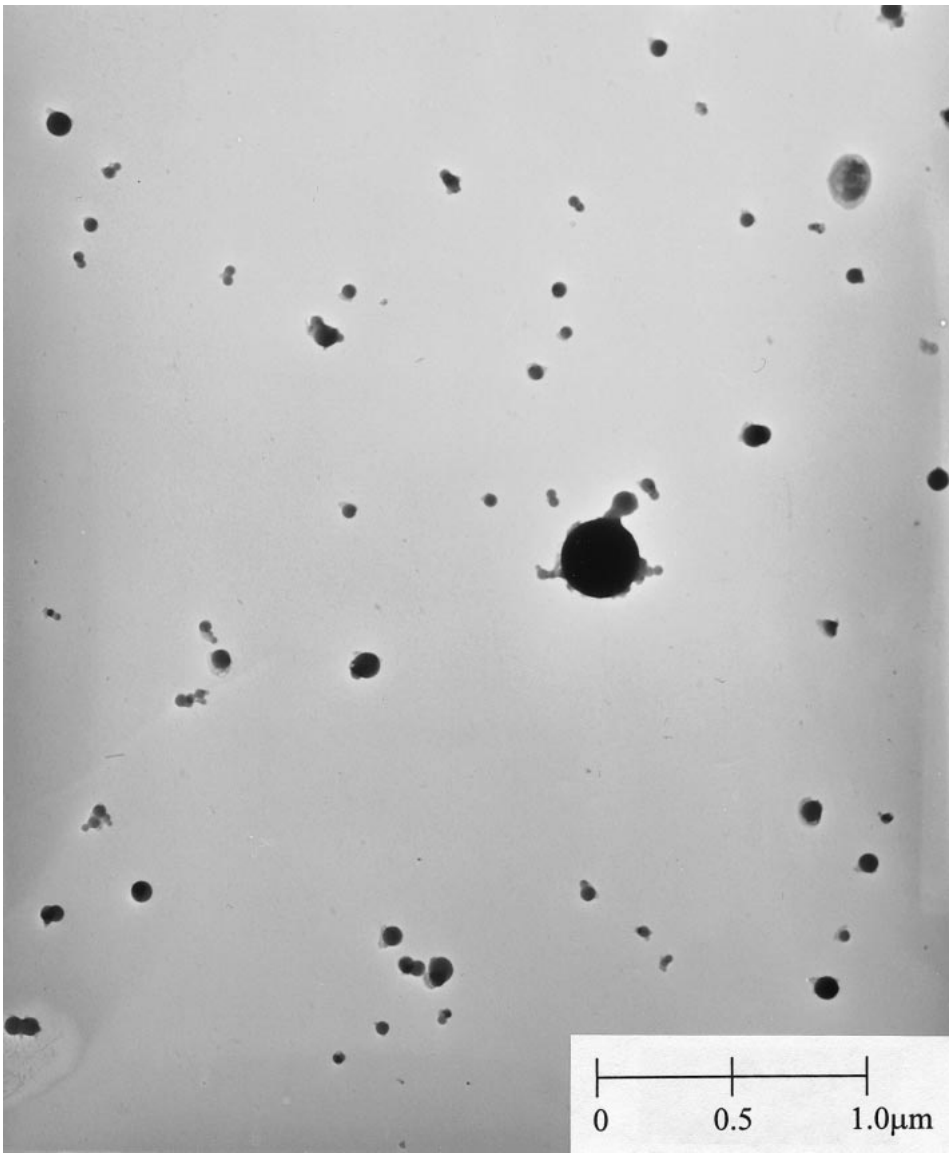

FIGURE 7. TEM photograph of the aerosols formed when the brazing alloy is used with a supplemental fluxing compound (900°C)

not be identified using this technique, because their atomic number was below the analytical detection limit (i.e., less than an atomic number = 11). The lack of agglomerates and the spherical nature of these aerosols confirms that nucleation followed by condensational growth were the dominant aerosol formation mechanisms.

Characteristic time calculations for the different processes also were calculated using the procedure described by Biswas and Wu.[30] The results indicate that the characteristic time for nucleation ($\sim 10^{-3}$ sec) is clearly lower than the residence time ($\sim$3 sec), thus the vapors are expected to nucleate to form particles. The characteristic time for condensation is approximately 0.1 sec, lower than that of the coagulation characteristic time ($\sim$100 sec).[20] Therefore, condensation is expected to be the dominant growth process, as indicated by earlier observations.

The sample results from these tests (V–VIII) suggest that the use of the supplemental fluxing compound resulted in a significant increase (greater than two orders of magnitude) in the total particle number concentration, and an increase in the number mean particle size. These results also suggest that these fumes resulted from the chemical interaction of chemical species within the fluxing compound and brazing alloy. These results suggest that during an actual brazing operation the supplemental fluxing compound would increase the generation of fumes significantly, thus increasing the potential hazard to the worker.

Equilibrium Analysis

The following section presents the results of the simulation cases that were used to assist in the interpretation of the furnace study results (Table II). Considering that brazing operations take place under high temperatures, and that chemical reaction rates tend to vary exponentially with temperature, the equilibrium assumption will yield reasonable qualitative estimates.

In Case A, the brazing metal alloy was tested by itself with varying quantities of phosphorus to determine its effect on chemical speciation. This case simulated using the alloy without the supplemental fluxing compound. Figures 8a and 9a illustrate the

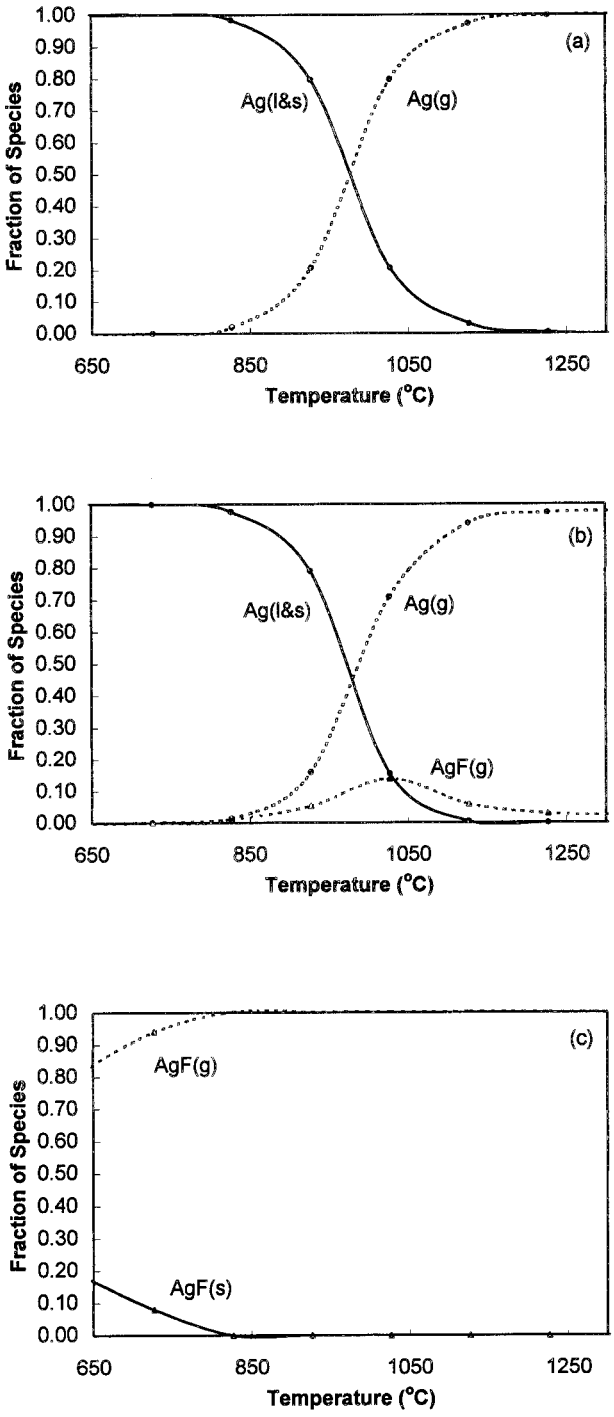

FIGURE 8. Thermodynamic equilibrium analysis results for the speciation of silver: (a) Case A, (b) Cases B and E, and (c) Cases C and D (see Table II) (s = solid, l = liquid, g = gas phase species)

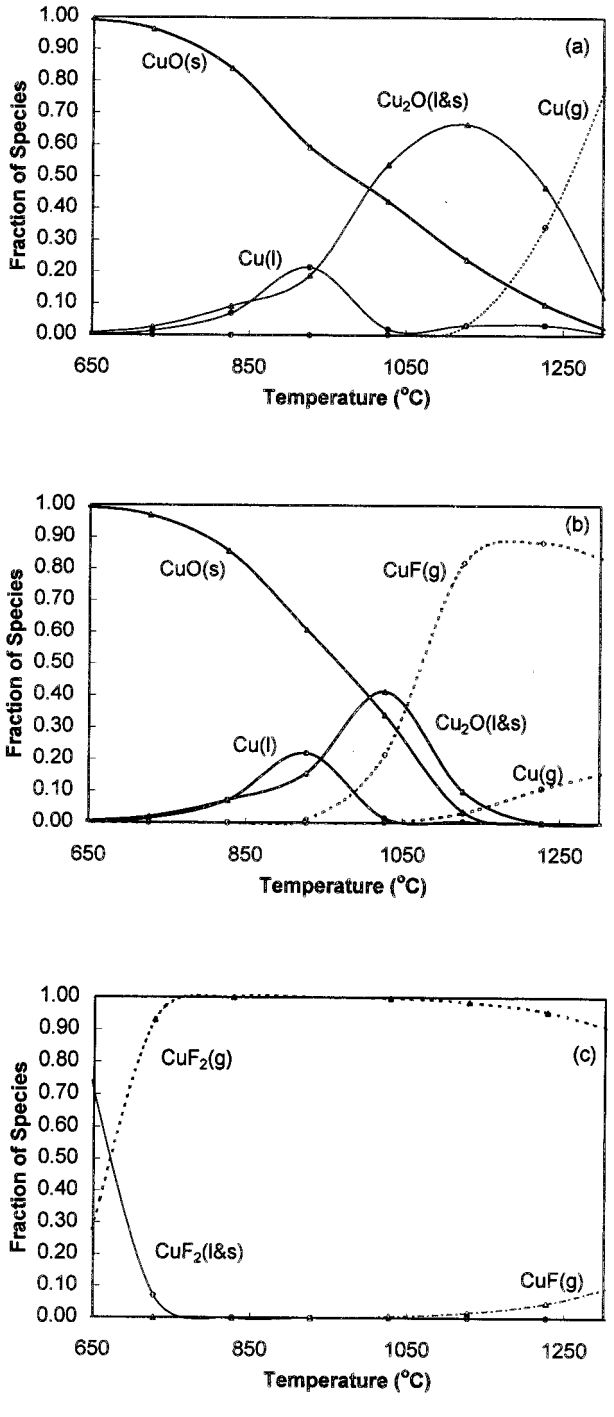

FIGURE 9. Thermodynamic equilibrium analysis results for the speciation of copper: (a) Case A, (b) Cases B and E, and (c) Cases C and D (see Table II) (s = solid, l = liquid, g = gas phase species)

equilibrium results for silver and copper, respectively. Phosphorus appeared to have no effect on the partitioning (between the gas and condensed phases) of either metal under the conditions tested. At temperatures greater than 1000°C, elemental silver is thermodynamically favored as a gas (Figure 8a). Below these temperatures, the condensed form (solid and liquid) of elemental silver is favored. At temperatures greater than 1250°C, elemental copper is the dominant species (Figure 9a). Below 1250°C, copper oxides in the condensed form are thermodynamically favored. In the temperature range (700–1000°C) evaluated during the furnace study, this analysis suggests that gas phase copper species were not present. Additionally, it appears that silver may have been present in its gaseous form at temperatures greater than 850°C, and would have become significant at temperatures greater than 1000°C. For

example, assuming 10^{-6} moles of silver were present in one mole of air at 1000°C, over half of the silver would be in the gas phase. As this vapor cools, aerosols form because the gas phase species is no longer thermodynamically favored at low temperatures. The use of phosphorus as a fluxing agent was clearly apparent in reacting with oxygen to form various oxide species including gaseous PO_2, P_4O_{10}, and P_4O_6. Therefore, the phosphorus protects the metal alloy from oxidation by forming P_xO_y species.

In Case B, fluoride was added to the simulation at molar quantities equal to that of the metals. This simulation was conducted to test the effect of fluoride on the metal speciation, and to determine the relative affinity of each metal for the fluoride. No hydrogen was added during this simulation. The silver speciation was affected by the fluoride at temperatures greater than 850°C (Figure 8b). Gaseous AgF reached a maximum value at 1030°C and comprised roughly 15% of the total silver species. It appears that the relative partitioning of the silver between the gaseous and condensed phases occurred in a manner similar to that of Case A. In contrast, copper was markedly affected by fluoride (Figure 9b). Case A demonstrated that without fluoride, gaseous elemental copper is dominant at temperatures greater than 1250°C. However, fluoride serves to reduce the temperature at which gas phase species become dominant. In this case, gaseous copper fluoride becomes dominant at temperatures greater than 1100°C. Assuming a furnace temperature of 1100°C, copper fluoride vapors would be present in the airstream, and would tend to form an aerosol on cooling (through dynamic processes such as nucleation, condensation, and coagulation). In contrast, without fluoride, gas phase copper species are not present at this temperature (Figure 9a). Another gaseous metal species predicted in these conditions was boron trifluoride (30% of total boron species from 600 to 800°C). This species is considered a severe pulmonary irritant (also a gas at room temperature), and has been associated with the use of fluxing compounds.[31] Under these simulation conditions, fluoride reacted readily with copper and boron, and to a lesser extent with silver. Due to the relative stability of silver, this finding appears reasonable.

In Case C, fluoride was added in excess quantities when compared with that of the metals. As demonstrated by Figures 8c and 9c, excess fluoride dramatically shifted the speciation to gaseous metal fluoride compounds. At 650°C, gaseous AgF comprised 84% of the total and increased to 100% of the total at 850°C (Figure 8c). At 650°C, gaseous CuF_2 comprised 30% of the total, rising to 100% of the total at 850°C (Figure 9c). Boron trifluoride comprised 100% of the total boron species throughout the entire temperature range. The remaining fluoride reacted with nitrogen and oxygen to form gaseous FNO. This species comprised roughly 30% of the total fluoride species from 650 to 1300°C. These results suggest that when added in excess quantities gaseous copper and silver fluorides are thermodynamically favorable, and will readily form aerosols when cooled. Cases B and C suggest that the fluoride in the fluxing compound will readily react with the metals in the brazing alloy (copper and silver) to form gas phase metal fluoride species. Based on the furnace study results, the use of the fluxing compound markedly increased the production of aerosols. The equilibrium results may provide an explanation for the differences noted when the alloy was used by itself and in conjunction with the fluxing compound.

In Cases D and E, fluoride was added in the same quantity as Case C. In Case D, hydrogen was added to the simulation at molar quantities equal to that of the metals. In Case E, hydrogen was added to the simulation in excess quantities when compared with that of the metals. In Case D, the fluoride speciation shifted such that FNO comprised 20% of the total fluoride, while FH comprised 10% of the total fluoride species. In Case D, the addition of hydrogen resulted in the same (within 5%) metal speciation as that of Case C (Figures 8c and 9c). When fluoride and hydrogen were added to the simulation in excess molar quantities (Case E), hydrogen fluoride was a major constituent. In Case E, fluoride reacted with copper and silver in a manner very similar to that of Case B (within 5%) (Figure 8b and 9b). Boron behaved slightly different from Case B in that gaseous BHO_2 contributed approximately 10% of the total boron species from 900 to 1200°C. These results show that hydrogen will tend to compete with the metals to form hydrogen fluoride, a severe pulmonary irritant.[31] As a result of this analysis, it appears that the formation of metal fluoride species will depend on (1) the metal, (2) the temperature, and (3) the amount of fluoride and hydrogen that is available for reaction. However, the equilibrium results clearly suggest that fluoride (a major ingredient in the fluxing compound) had reacted with the silver and copper in the brazing alloy to form metal fluoride species.

Implications

Brazing operations frequently are conducted using a furnace or torch. The alloys used in brazing are designed to have melting points lower than that of the base metals, and in some cases (i.e., the alloy used in this study) are also designed to prevent oxidation at the molten metal surface. This study demonstrated several findings, including the time before the onset of oxidation. For a furnace operation, if brazing is carried out in an inert environment (e.g., nitrogen), oxidation is not a problem. In this situation, the fumes generated are transient (~300 sec) and primarily consist of ultrafine phosphorus species that behave in a similar manner over a wide temperature range (Figure 4). For furnace operations conducted in an air environment, the fumes generated (alloy only) are also transient and associated with the generation ultrafine phosphorus species (oxide and metal). Unlike the fumes generated under inert conditions, the fumes generated in an air environment will tend to increase with an increase in temperature (Figure 3). When the molten alloy is exposed to air, this study demonstrated that the volatilization of the phosphorus species (and the subsequent formation of aerosols) is transient. As time progresses, phosphorus in the alloy is consumed, allowing oxidation to occur at the molten metal surface. From a metallurgical standpoint, the temperature and the time of heating the alloy should be minimized to prevent oxidation from occurring. For example, oxidation of the molten metal surface will occur in less than 600 sec with a furnace temperature of 900° (Figures 3 and 5).

When a torch is used, the time-temperature history is more complex. First, local temperatures can be significantly higher, and the brazing is also taking place in an air environment. An experienced brazer is careful to limit both the temperature and time of heating the alloy because either condition will tend to consume phosphorus within the alloy, thereby promoting oxidation at the molten metal surface.[11,13] Therefore, the metal should be heated in a manner that approaches the flow point temperature of the alloy (732°C). It should be noted that flame temperatures can be very high (ranging from 1200 to 2200°C) and in such cases, the time available before oxidation occurs is shorter.

In a brazing operation in which the alloy is used by itself, an ultrafine aerosol will be generated. The aerosols generated under these conditions are transient and appear to be associated with phosphorus species. The volatilization of these species prevents

oxidation at the molten metal surface, thus demonstrating the efficacy of phosphorus as a fluxing agent. In contrast, when the brazing alloy is used with the supplemental fluxing compound, the fumes generated are relatively nontransient, orders of magnitude higher in concentration, and are associated with the formation of metal fluoride species (Table III, Figure 8 and Figure 9). From an occupational standpoint, brazing operations should take place using low temperatures (above the alloy flow point) to minimize volatilization from the molten metal surface. In addition, this alloy should be used without the supplemental fluxing compound (whenever possible, the self-fluxing alloy is better in this regard) to reduce occupational exposures to brazing fumes.

CONCLUSIONS

When the alloy is used by itself, the results of the furnace study suggest that the aerosols formed were transient and were mainly associated with mass transfer of phosphorus species from the molten metal surface to the surrounding gas. These results demonstrate the utility of phosphorus as a fluxing compound. In contrast, when this alloy is used in conjunction with the fluxing compound, a relatively stable, submicron-size aerosol was generated that was several orders of magnitude higher in concentration when compared with the ''alloy alone'' sample results. Thermodynamic equilibrium analysis suggested that fluoride (a major constituent in the fluxing compound) played a significant role in reacting with the brazing alloy metals to form gas phase metal fluoride compounds. These gas phase metal species have vapor pressures that are significantly higher than either the elemental or oxide metal species, and would volatilize readily from the molten metal surface. As these metal-fluoride vapors cool, submicron fumes were formed mainly through nucleation and condensation growth processes. In addition, the equilibrium results revealed the potential formation of severe pulmonary irritants (HF and BF_3) from heating the supplemental fluxing compound. Using this methodology, an occupational health professional could evaluate the potential toxicity of a wide variety of welding alloys and fluxing compounds. The furnace study and equilibrium results demonstrate the importance of fluxing compounds in the formation of brazing fumes, and suggest that fluxing compounds can be selected that serve their metallurgical intention and suppress the formation of aerosols.

REFERENCES

1. **Connor, L.P. (ed.):** *Welding Handbook,* 8th ed., vol. 1. Miami, Fla.: American Welding Society, 1987. pp. 2–30.
2. **National Institute for Occupational Safety and Health (NIOSH):** *NIOSH Criteria for a Recommended Standard: Welding, Brazing, and Thermal Cutting,* (DHHS [NIOSH] Pub. no. 88–110). Cincinnati, Ohio: NIOSH, 1988. pp. 25–35, 39–55, 104–111.
3. **American Welding Society (AWS):** *Fumes and Gases in the Welding Environment.* Miami, Fla.: AWS, 1979. pp. 63–86.
4. **Hewitt, P.J., R. Hicks, and H.F. Lam:** The generation and characterization of welding fumes for toxicological investigations. *Ann. Occup. Hyg. 21*:159–167 (1978).
5. **Bureau of the Census:** Detailed population characteristics. In *1980 Census of Population,* vol. 1. Washington, D.C.: U.S. Department of Commerce, Bureau of the Census, 1984.
6. **Heile, R.R., and D.C. Hill:** Particulate fume generation in arc welding processes. *Welding J.* 54(7):201s–210s (1975).
7. **Hewett, P.:** The particle size distribution, density, and specific surface area of welding fumes from SMAW and GMAW mild and stainless steel consumables. *Am. Ind. Hyg. Assoc. J. 56*:128–135 (1995).
8. **Donaldson, K., P. Gilmour, D.M. Brown, H. Beswick, et al:** Surface free radical activity of pm10 and ultrafine titanium dioxide: A unifying factor in their toxicity. In *Inhaled Particles VIII,* T.L. Ogden (ed.) Elmsford, N.Y.: Pergamon Press, 1998.
9. **Takenaka, S., H. Dornhofer-Takenaka, and H. Muhle:** Aveolar distribution of fly ash and titanium dioxide after long-term inhalation by Wistar rats. *J. Aerosol Sci. 17*:361–364 (1986).
10. **Ferin, J., G. Oderdorster, S. Penney, S.C. Soderholm, et al**: Increased pulmonary toxicity of ultrafine particles? I. Particle clearance, translocation, morphology. *J. Aerosol Sci. 21*:381–384 (1990).
11. **Rupert, W.D.:** Copper-phosphorus alloys offer advantages in brazing copper. *Welding J. 5*:43–45 (1996).
12. **Rupert, W.D.:** Braze life after cadmium. *Welding J. 11*:59–61 (1995).
13. **Ballentine, R.E.:** Silver's role in phosphorus-copper brazing filler metals. *Welding J. 10*:41–42 (1994).
14. **Lin, W.Y., and P. Biswas:** Metallic particle formation and growth dynamics during incineration. *Combust. Sci. Technol. 101*:29–43 (1994).
15. **Wu, C.Y., and P. Biswas:** An equilibrium analysis to determine the speciation of metals in an incinerator. *Combust. Flame 93*:31–40 (1993).
16. **Fernandez, M.A., L. Martinez, M. Segarra, J.C. Garcia, F. Espiell:** Behavior of heavy metals in the combustion gases of urban waste incinerators. *Environ. Sci. Technol. 26*:1040–1047 (1992).
17. **Durlak, S.K., P. Biswas, and J. Shi:** Equilibrium analysis of the affect of temperature, moisture and sodium content on heavy metal emissions from municipal solid waste incinerators. *J. Haz. Mat. 56*:1–20 (1997).
18. **Owens, T.M., C.Y. Wu, and P. Biswas:** An equilibrium analysis for reaction of metal compounds with sorbents in high temperature systems. *Chem. Eng. Comm. 133*:31–52 (1995).
19. **Nishida, T., Kimura, K., and Inagaki, M.:** Behavior of cadmium on brazing. *Quart. J. Japan Welding 12*:485–494 (1994).
20. **Zimmer, A.T.:** ''Mechanistic Understanding of Aerosol Emissions from Brazing Operations.'' MS thesis, University of Cincinnati, 1998.
21. **Biswas, P., X. Li, and S.E. Pratsinis:** Optical waveguide preform fabrication. *J. Appl. Phys. 65*:2445–2451 (1989).
22. **Wang, S.C., and R.C. Flagan:** Scanning electrical mobility spectrometer. *Aerosol Sci. Technol. 13*:230–240 (1990).
23. **White, W.B., S.M. Johnson, and G.B. Dantzig:** Chemical equilibrium in complex mixtures. *J. Chem. Phys. 28*:751–756 (1958).
24. **Gray, C.N.:** ''Fume Formation in Electric Arc Welding.'' PhD dissertation, University of Bradford, U.K. 1980.
25. **Levenspiel, O.:** *Chemical Reaction Engineering.* New York: John Wiley & Sons, 1993.
26. **Reynolds, W.:** *STANJAN—Interactive Computer Programs for Chemical Equilibrium Analysis* [Computer software]. Stanford, Calif.: Stanford University, 1990.
27. **Chase, M.W., C.A. Davies, J.R. Downey, D.J. Frurip, et al:** *JANAF Thermochemical Tables.* Midland, MI: American Chemical Society and American Institute of Physics for the National Bureau of Standards, 1986.
28. **Wiedensohler, A.:** An approximation of the bipolar charge distribution for particles in the submicron range. *J. Aerosol Sci. 19*:387–390 (1988).
29. **TSI Inc.:** *Instruction Manual: Model 3022A Condensation Particle Counter.* St. Paul, Minn.: TSI Inc., 1994.
30. **Biswas, P., and Wu, C.Y.:** Control of toxic emissions from combustors using sorbents: A review. *J. Air Waste Manage. Assoc. 48*:113–127 (1998).
31. **American Conference of Governmental Industrial Hygienists (ACGIH):** *Documentation of the Threshold Limit Values and Biological Exposure Indices,* 6th ed. Cincinnati, Ohio: ACGIH, 1991.